Journal of Applied Polymer Science

Synthesis of Functional Poly(styrene)-*block*-(methyl methacrylate/methacrylic acid) by Homogeneous Reverse Atom Transfer Radical Polymerization: Spherical Nanoparticles, Thermal Behavior, Self-Aggregation, and Morphological Properties

Guadalupe del C. Pizarro,[1] Manuel Jeria-Orell,[1] Oscar G. Marambio,[1] Andrés F. Olea,[2] Daniela T. Valdés,[1] Kurt E. Geckeler[3,4]

[1]Departamento de Química, Universidad Tecnológica Metropolitana. Santiago, Chile

[2]Departamento de Ciencias Químicas, Facultad de Ciencias Exactas, Universidad Andrés Bello, Los Fresnos 52, Viña del Mar, Chile

[3]Department of Nanobio Materials and Electronics (WCU), Gwangju Institute of Science and Technology (GIST), Gwangju 500-712, South Korea

[4]Laboratory of Applied Macromolecular Chemistry, School of Materials Science and Engineering, Gwangju Institute of Science and Technology (GIST), Gwangju, South Korea

Correspondence to: G. d. C. Pizarro (E-mail: gpizarro@utem.cl)

ABSTRACT: This study investigates the use of homogeneous reverse atom transfer radical polymerization for the synthesis of polystyrene (PS) initiated by conventional radical peroxide with copper bromide in the lower oxidation state and a 2,2′-bypyridine complex as the catalyst. In a second stage, an amphiphilic block copolymer containing methyl methacrylate (MMA) was synthesized via normal atom transfer radical polymerization in two steps, followed by partial hydrolysis of the methyl ester linkage of the MMA block under acidic conditions. The block copolymer PS_{699}-*b*-P(MMA_{232}/MAA_{58}) obtained had a narrow molecular weight dispersity ($Đ < 1.3$). The structure of the precursor, PS-*b*-PMMA, and resultant polymer, was characterized and verified by FTIR and ^{1}H-NMR spectroscopy as well as size exclusion chromatography. The self-aggregation of PS_{699}-*b*-P(MMA_{232}/MAA_{58}) in organic solvents was monitored by UV spectroscopy, whereas the morphology and size of the formed microaggregates were investigated by transmission electron microscopy and dynamic light scattering. The results indicate that this copolymer formed regular spherical reverse micelles with a core–shell structure. The atomic force micrographs of PS_{699}-*b*-P(MMA_{232}/MAA_{58}) showed a rough surface morphology owing to microphase separation of the block copolymer. In addition, thermal characterization was performed by differential scanning calorimetry and thermogravimetric analysis. The glass transition temperature of PS_{699}-*b*-P(MMA_{232}/MAA_{58}) decreased significantly (65°C), when compared to PS and PMMA, suggesting that an enhanced movement of the polymer chains resulted by the segregation of the hydrolyzed P(MMA_{232}/MAA_{58}) block. © 2013 Wiley Periodicals, Inc. J. Appl. Polym. Sci. 129: 2076–2085, 2013

KEYWORDS: micelles; morphology; nanostructured polymers; phase behavior; properties and characterization

Received 8 October 2012; accepted 11 December 2012; published online 7 January 2013
DOI: 10.1002/app.38923

INTRODUCTION

During the last decade, significant advancement has been made in the area of controlled free-radical polymerization, including atom transfer radical polymerization (ATRP), offering new synthesis routes to obtain well-defined polymers with low dispersities[1] for applications ranging from next-generation separation media[2,3] to controlled release vehicles,[4,5] catalyst supports,[6] and nanoreactors.[7] ATRP has been successfully employed for the polymerization of a variety of monomers, such as styrene and its derivatives,[8] acrylates and methacrylates,[9–11] using a copper-based system and producing well-defined polymers in a relatively short period of time. There are several reports on the synthesis of amphiphilic block copolymers and the study of their properties, as these copolymers are important materials in the several fields of natural science, for example, colloid science and biochemistry, as well as in industrial fields.[12–15]

In a normal ATRP reaction, the initiating radicals are generated from an alkyl halide in the presence of a transition metal in its

lower oxidation state; however, conventional radical initiators, such as azobisisobutyronitrile (AIBN) or benzoyl peroxide (BPO), can also be employed. The latter approach is known as reverse ATRP and has been successfully used for copper-based heterogeneous and homogeneous systems.[16,17]

It has also been observed that reverse ATRP initiated by peroxides sometimes proceeds quite differently than in cases when using azo compounds. The differences between the BPO and the AIBN systems have been ascribed to an electron transfer and the formation of copper benzoate species.[17,18] For instance, the polymerization of the homogeneous BPO/$CuBr_2$/$(dNbpy)_2$ system cannot be controlled.[19] In contrast, a controlled living polymerization has been observed when BPO was used in conjunction with CuBr/$(dNby)_2$.[20] In a heterogeneous system, where 2,2′-bipyridine (Bpy) is employed as the ligand, both CuBr and $CuBr_2$ lead to a controlled polymerization of styrene. On the other hand, the controlled polymerization of methacrylic acid (MAA) by ATRP is challenging owing to acid monomers poisoning the catalysts by coordinating to the transition metal. In this way, poly(methacrylic acids) can be prepared by polymerization of protected monomers such as trimethylsilyl methacrylate, *tert*-butyl methacrylate, tetrahydropyranyl methacrylate, and benzyl methacrylate.[21]

In this context, the purpose of this study has been to investigate the use of homogeneous reverse ATRP for the synthesis of polystyrene (PS) initiated by the conventional radical initiator peroxide BPO, copper bromide complexes in the lower oxidation state (CuBr), and with Bpy as the ligand. Then, a block copolymer containing methyl methacrylate (MMA) was synthesized via normal ATRP initiated by PS-Br/CuBr/Bpy. In this procedure, the activator species (R–X) were generated *in situ* by reactions triggered by the decomposition of conventional free-radical initiators.[16,17]

The block copolymer was synthesized by a two-step ATRP, and hence the molecular weight could be controlled by varying the feeding ratio or monomer conversion. The ATRP process exhibited a good control of the polymer molecular weights, giving high conversion and a dispersity of <1.3. Finally, the hydrolysis of MMA block was performed under acid conditions. The use of MMA as the monomer to build the poly(methacrylic acid) backbone was explored (Scheme 1). The reasons for employing this methodology include the synthetic advantages of this system: components that are less sensitive to air, and the possibility to obtain diblock copolymers with controlled molecular weights and low dispersity. In addition, the precursors of the catalyst system are easier to handle and the procedure is compatible with commercial processes.

The block copolymers were characterized by FTIR and ^{1}H-NMR spectroscopy as well as size exclusion chromatography (SEC). Subsequently, the self-assembly behavior of these copolymers in organic solvents was investigated by the absorption probing method, whereas the size and morphology of the formed aggregates were studied by transmission electron microscopy (TEM) and dynamic light scattering (DLS). The results indicated that the amphiphilic diblock copolymer self-assembled into reverse micelles, depending on the length of both blocks.

EXPERIMENTAL

Materials

Styrene (Sigma-Aldrich Chemicals, Germany) was washed with 5% aqueous NaOH solution to remove any inhibitor, and was then distilled under reduced pressure prior to use. Methyl methacrylate (Merck-Schuchardt Chemicals, Germany) was purified by distillation under reduced pressure.

BPO (Merck-Schuchardt, with 25% H_2O, Germany) was used as received. Copper(I) bromide (Aldrich, 98%) was purified by

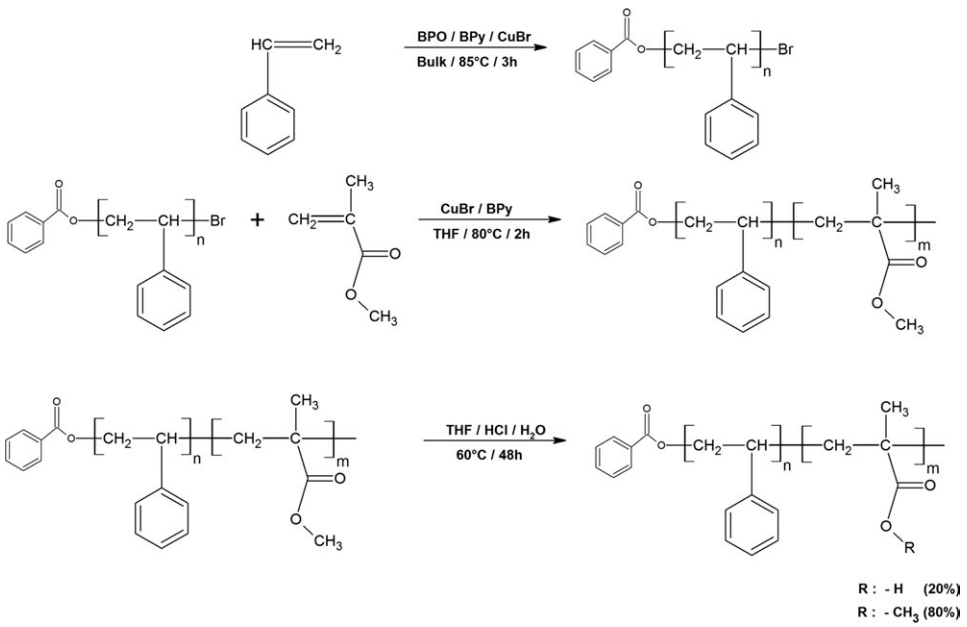

Scheme 1. Synthesis of the PS_{699}-*b*-P(MMA_{232}/MAA_{58}) copolymers by ATRP: (a) reverse ATRP and (b) normal ATRP.

stirring overnight over acetic acid at room temperature, followed by washing the solid with ethanol and diethyl ether prior to drying at 50°C under vacuum for 1 day. 2,2′-Bipyridyl (Sigma-Aldrich, 99%) was used as received.

Characterization of the Block Copolymers

FTIR spectra were recorded on a Bruker Vector 22 spectrometer (Bruker Optics GmbH, Ettlingen, Germany). ^{1}H-NMR spectra were recorded in solution at room temperature with a Bruker AC 250 spectrometer (Bruker, Karlsruhe, Germany) using deuterated chloroform ($CDCl_3$, 99.8%) as the solvent.

Determination of the Molecular Weight

The number average (M_n) and weight average (M_w) molecular weight were determined by SEC under the following conditions: WATERS 600E instrument equipped with UV and RI detectors, using tetrahydrofuran (THF) as the solvent (flow rate: 1.0 mL min^{-1}). The samples were measured at 30°C at a concentration of 6 mg mL^{-1}, and the calibration was performed using PS standards. From these data, the molecular weight distribution or dispersity, $Đ = M_w/M_n$ was calculated.

Thermal Behavior

The thermal stability and glass transition temperatures (T_g) of the copolymers were determined by thermal gravimetric analysis (TGA) and differential scanning calorimetry (DSC) (Mettler Toledo Star System 822e). Thermograms were recorded under a nitrogen atmosphere at a heating rate of 10°C min^{-1}. Samples of 3–4 ± 0.1 mg were used in each experiment. To eliminate the effect of thermal history on the phase transitions, all samples were heated to 150°C, held at that temperature for 5 min, and then cooled to 30°C.

Morphological Properties of the Polymer Aggregates

The morphology of aggregates formed in organic solvents was investigated by TEM and scanning electron microscopy (SEM). The samples of PS_{699}-*b*-P(MMA_{232}/MAA_{58}) were dissolved in THF at concentrations of 0.15 and 0.1%, and these solutions were subsequently spin-coated (RC5, Suess Microtec, Garching, Germany). TEM (JEOL JEM 1200EX, operating at 120 kV, with a point resolution of approximately 4 Å) and SEM (JEOL, JSM-6380LV) were performed on the dispersed samples. The TEM images were captured by placing a drop of the THF solution onto a carbon-coated copper grid. The surface characterization of block copolymers was carried out by employing atomic force microscopy (AFM) (Digital Instruments NanoScope IIIA Series employed in "tapping" mode at a scan rate of 10.0 mm s^{-1}).

DLS Measurements

The size dispersion (effective diameter, nm), and size distribution (dispersity) of the polymer aggregates in THF were determined by DLS measurements (Particle Size Analyzer, Nano DLS, Brookhaven Instruments, Holtsville, NY, USA, equipped with "90 Plus Particle Sizing Software ver. 3.74"). Samples with a concentration of 1 mg mL^{-1} were prepared by direct dissolution of the block copolymer in THF. The DLS measurements were performed at 25°C at a scattering angle of 90°, employing nanospheres of PS with an effective diameter of 90 nm.

Absorbance Measurement

The absorbance spectrum of methylene blue (MB, $C_{16}H_{18}N_3SCl$) in toluene, in the presence of different concentrations of PS_{699}-*b*-P(MMA_{232}/MAA_{58}) (range, 0.04–0.4 mg mL^{-1}) was recorded at 25°C between 400 and 800 nm in a Shimadzu UV-1700 spectrophotometer.

Synthesis of PS–Br Macroinitiator by Reverse ATRP

The macroinitiator, PS–Br, was obtained by reverse ATRP in the bulk using BPO/CuBr/Bpy as the catalyst system. In a typical polymerization experiment, a mixture of 49.8 mg BPO (0.206 mmol), 29.6 mg CuBr (0.206 mmol), and 64.5 mg Bpy (0.413 mmol) was added to a Schlenk flask. The oxygen was removed by three freeze–vacuum–thaw cycles (1.33×10^{-4} kPa). Then, 5 mL of styrene (43.3 mmol) was added under a nitrogen atmosphere, and the mixture was heated at 85°C for 3 h. The polymerization was terminated by immersing the flask into liquid nitrogen. The product was dissolved in THF, and the solution was passed through a silica column to remove the copper catalyst. The resulting solution was precipitated in methanol, and then dried at 60°C under vacuum to a constant weight. The product was PS–Br (yield: 40%, $M_n = 7.3 \times 10^4$ g mol^{-1}, $Đ = 1.28$), and its ^{1}H-NMR spectra ($CDCl_3$; δ ppm) exhibited the following signals: 1.2–2.0 [2H, —CH_2; and 1H, —CH from the backbone]; and 6.2–7.3 [5H, —Ar] [Figure 1(a)]. The FTIR spectrum (KBr, cm^{-1}) for PS–Br illustrated the following absorption bands: 3024 and 2921cm^{-1} [υ(CH, CH_2)]; and 754–699 cm^{-1} [υ(CH—, aromatic ring)] [Figure 2(a)].

Synthesis of PS-*b*-PMMA by Normal ATRP

PS-*b*-PMMA copolymer was synthesized using MMA/PS-Br / CuBr/BPy, in a mole ratio of 100/1/1/2. In a typical experiment, 6080 mg of the macroinitiator (0.0833 mmol $M_n = 7.3 \times 10^4$) was charged to a Schlenk flask and dissolved in THF, after which 833 mg of MMA monomer (8.33 mmol) and 26.0 mg of BPy (0.166 mmol) were added. The mixture was degassed by three freeze–vacuum–thaw cycles. Under agitation, 11.9 mg CuBr (0.0833 mmol) was added to the system over a time period of 20 min, and placed in an oil bath at a controlled temperature of 80°C. After 2 h, the reaction was stopped by immersing the polymerization flask into liquid nitrogen. After the completion of the polymerization, the polymer solution was diluted with 10 mL THF, and then precipitated into methanol after passing through a silica column to completely remove the catalyst. The white powder obtained was purified by redissolution in THF and reprecipitation in methanol, and then dried at 60°C under vacuum. The product was dried until a constant weight was reached. The yield was found to be 68.8%, and the molecular weight and dispersity of PS-*b*-PMMA were 10.2 × 104 g mol^{-1} and 1.30, respectively. The ^{1}H-NMR spectra ($CDCl_3$; δ ppm) of this polymer showed the following resonance signals: 0.7–1.2 [3H, —CH_3]; 1.2–1.6 [2H, —CH_2]; 1.7–2.2 [2H, —CH_2, 1H, —CH]; 3.6–3.7 [3H, —CH_3 from the ester]; and 6.2–7.3 [5H, —Ar] [Figure 1(b)]. The weight contents of PS (65%) and PMMA (35%) in the block copolymer were calculated by ^{1}H-NMR from the ratio of the peak area of

the —CH_3 protons (a) at 0.8 ppm and aromatic protons (f, g) at 6.6 and 7.1 ppm [Figure 1(b,c)]. The FTIR spectrum (KBr, cm^{-1}) of PS-*b*-PMMA exhibited the most characteristic absorption bands: at 3007.3 and 2921.7 cm^{-1} [υ(CH, CH_2)]; at 1731 and 1633.7 cm^{-1} [υ(—C=O, ester)], and at 754.1 and 697.2 cm^{-1} [υ(aromatic ring)] [Figure 2(b)].

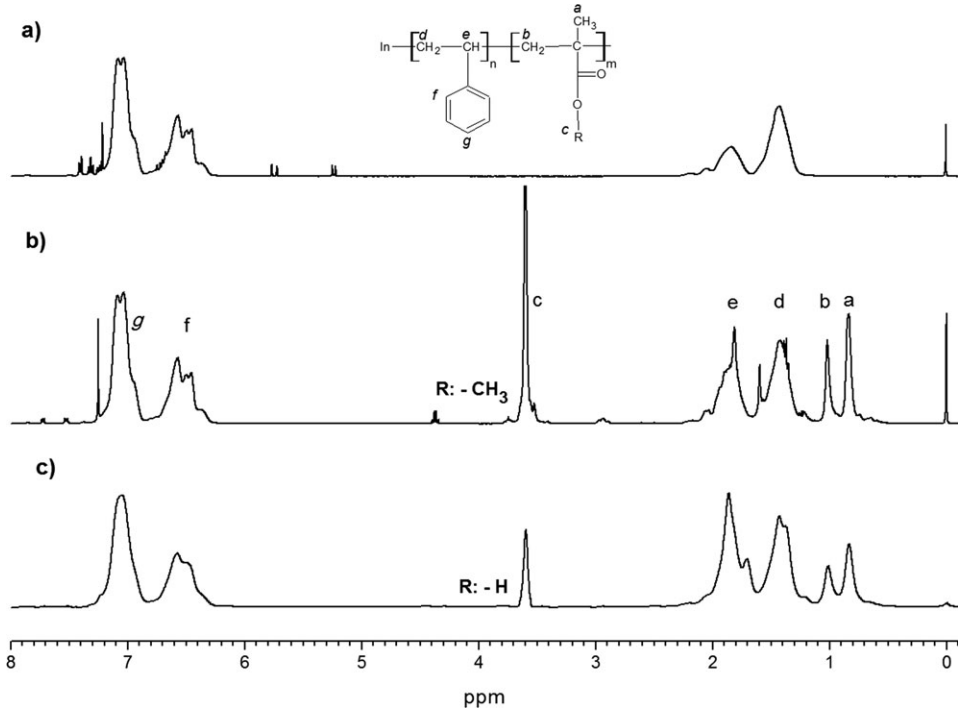

Figure 1. ^{1}H NMR spectra in $CDCl_3$ for (a) PS–Br, (b) PS_{699}-*b*-$PMMA_{290}$, and (c) PS_{699}-*b*-P(MMA_{232}/MAA_{58}).

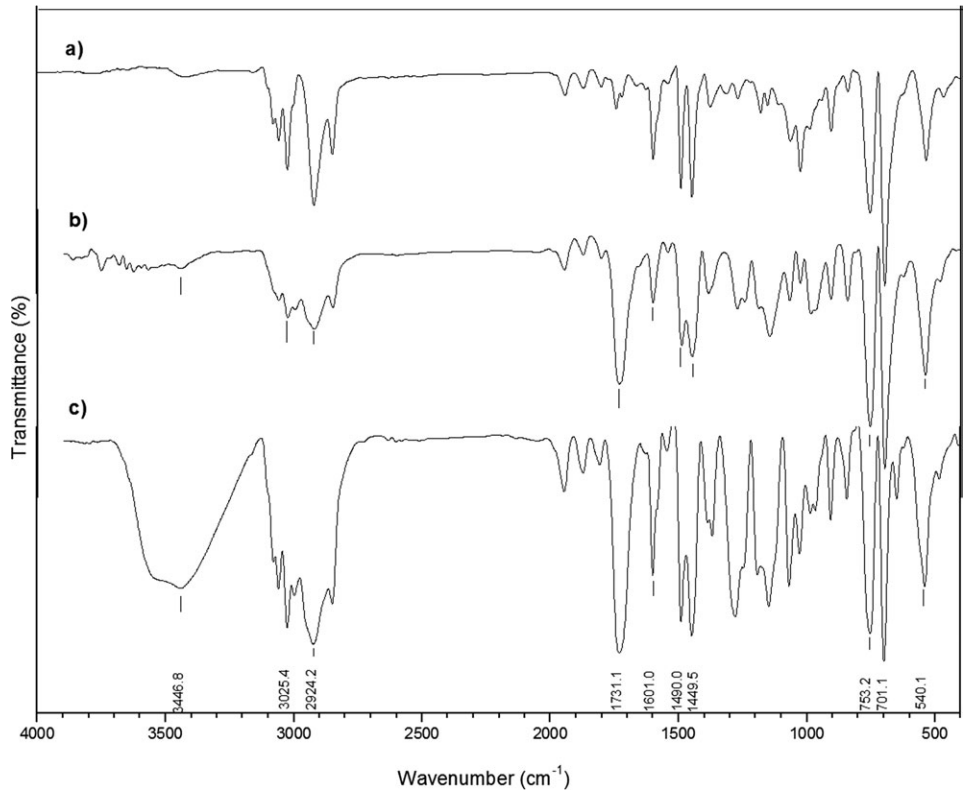

Figure 2. FTIR spectra of (a) PS–Br, (b) PS_{699}-*b*-$PMMA_{290}$, and (c) PS_{699}-*b*-P(MMA_{232}/MAA_{58}).

Table I. Thermal Behavior and Weight Loss for the Macroinitiator and Block Copolymers[a]

Samples	Copolymer composition (%) PS/PMMA/MAA	TDT_1 TDT_2 (°C)	Weight loss (%) at different temperatures (°C)				
			100	200	300	400	500
PS-Br	100	418	0.7	1.0	2.9	26.4	98.7
PS_{699}-*b*-$PMMA_{290}$	65 : 35	290–350	0.1	1.4	5.4	37.8	99.3
PS_{699}-*b*-P(MMA_{232}/MAA_{58})	65 : 29:6	180–388	0.7	8.4	15.6	38.6	99.8

[a] TDT, extrapolated thermal decomposition temperature.

Hydrolysis of the PMMA Block

PS-*b*-PMMA (0.500 g) was dissolved in THF (20 mL) and treated with an aqueous solution of HCl (25 mL) at 60°C for 48 h. Following the reaction, the solution was neutralized with an aqueous solution of NaOH. The organic phase was washed with water and dried over $MgSO_4$ overnight. After filtration, the solution was concentrated and precipitated into hexane. The hydrolysis product was dried under vacuum.

RESULTS AND DISCUSSION

A diblock copolymer of PS and PMMA was obtained in a two-step ATRP synthesis. Then, a hydrophilic poly(methacrylic acid) backbone was introduced to the polymer chain by hydrolysis of the PMMA block under acidic conditions. The synthetic route is shown in Scheme 1.

Synthesis of Macroinitiator and Block Copolymer

In the first stage, the macroinitiator PS–Br was prepared in bulk by reverse ATRP using BPO/CuBr/Bpy as the initiating system.[8–10] The obtained PS–Br was soluble in THF, with M_n = 7.3 × 10^4 g mol^{-1} and a relatively small dispersity, $Đ$ = 1.28, indicating a slow exchange between active and dormant species. In the second stage, a block copolymer, PS-*b*-PMMA, was prepared by normal ATRP with molecular weight equals to 10.2 × 10^4 g mol^{-1}. By using the molecular weight determined previously for PS (73,000 g mol^{-1}), the molecular weight of the second block was obtained to be 29,000 g mol^{-1}. Thus, the degree of polymerization determined by SEC is DP_n = 699 for PS and DP_n = 290 for PMMA. The weight contents of PS (65%) and PMMA (35%) in the block copolymer were confirmed by ^{1}H-NMR.

These results confirm that a polymer with a controlled molecular weight and narrow molecular weight distribution, PS_{699}-*b*-$PMMA_{290}$, had been obtained by ATRP.

Finally, an amphiphilic segment was introduced into the PS_{699}-*b*-$PMMA_{290}$ polymer chain by partial hydrolysis of the methyl ester linkage in the PMMA block under acidic conditions. The resulting copolymer was characterized by FTIR and ^{1}H-NMR spectroscopy. The formation of carboxylic group was confirmed by a broad absorption band at 3424.3 cm^{-1} in the FTIR spectrum [Figures 1(c) and 2(c)]. On the other hand, the NMR spectra ($CDCl_3$; δ ppm) of the hydrolyzed block copolymer showed a 20% decrease of the intensity of the signals appearing

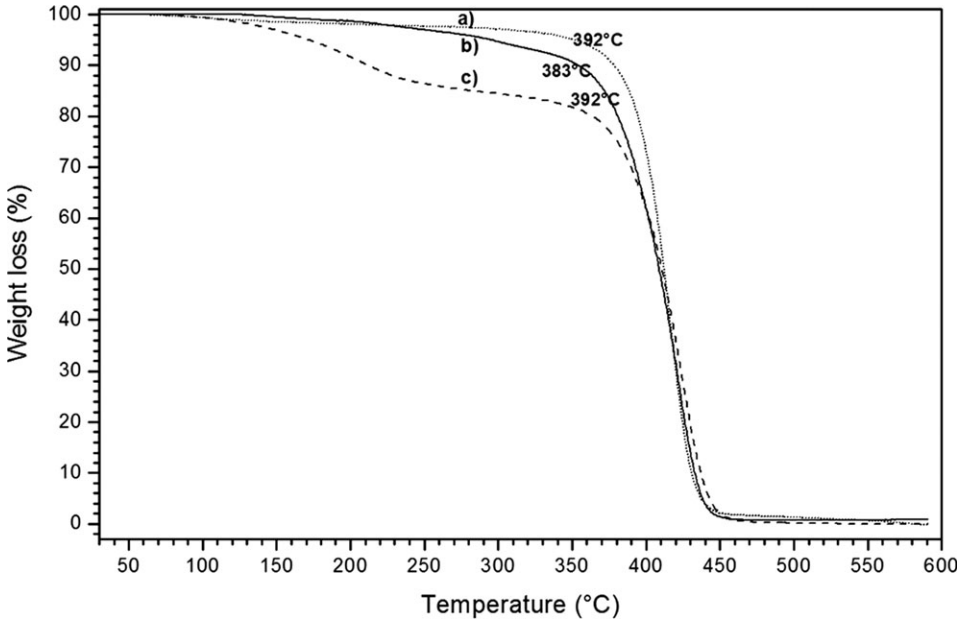

Figure 3. TGA thermograms of (a) PS–Br, (b) PS_{699}-*b*-$PMMA_{290}$, and (c) PS_{699}-*b*-P(MMA_{232}/MAA_{58}). Heating rate: 10°C min^{-1}.

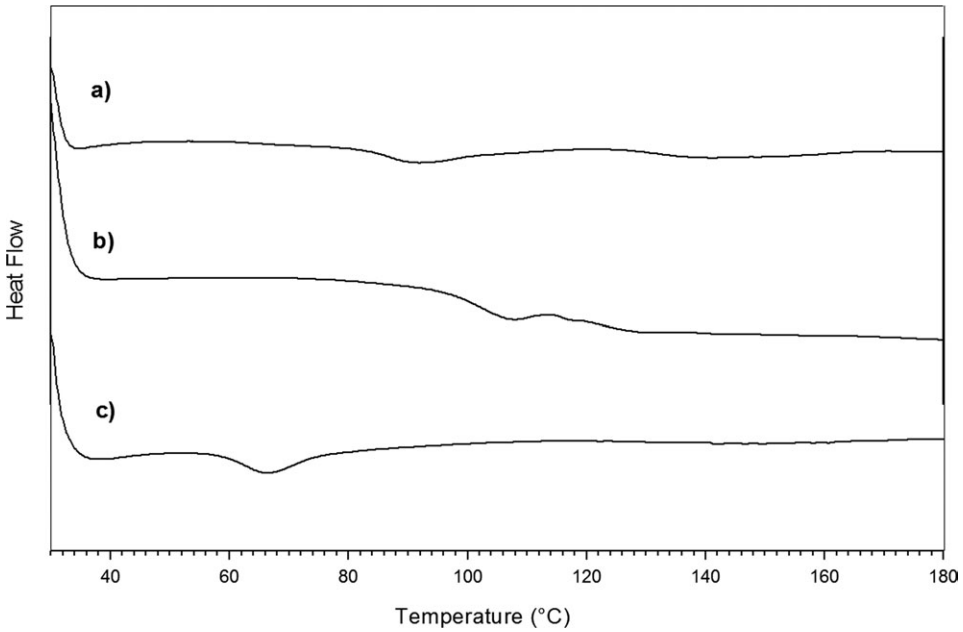

Figure 4. DSC thermograms of (a) PS–Br, (b) PS_{699}-*b*-$PMMA_{290}$, and (c) PS_{699}-*b*-$P(MMA_{232}/MAA_{58})$. Heating rate: 10°C min^{-1}.

at 3.5–3.6 ppm [—CH_3 ester protons of the PMMA block], which corresponds to the hydrolysis percentage of the methyl ester (leading to the formation of —COOH groups). This hydrolysis percentage indicates that 58 repeat units of the MMA units have been randomly transformed into MAA units. According to this, the structural formula of the resulting copolymer is PS_{699}-*b*-$P(MMA_{232}/MAA_{58})$.

Thermal Behavior

The thermal decomposition of the macroinitiator, precursor copolymer, and PS_{699}-*b*-$P(MMA_{232}/MAA_{58})$ was studied by TGA and DSC. The TGA results are summarized in Table I. The block copolymers exhibited a two-step degradation starting at 220 and 350°C. These thermal decomposition temperatures (TDTs) were lower than that of the macroinitiator (Figure 3). The PS–Br demonstrated a pronounced one-step degradation with TDT_1, equals to 418°C, whereas the block copolymer, PS_{699}-*b*-$PMMA_{290}$, exhibited a less significant two-step degradation. The first step, appearing between 250 and 300°C, was attributed to the decomposition of the PMMA segment, whereas the second step, over 390°C, may have been owing to the PS segment of the backbone chain. Furthermore, PS_{699}-*b*-$P(MMA_{232}/MAA_{58})$ displayed a two-step degradation (Figure 3) but was less stable than the precursor copolymer. The first step,

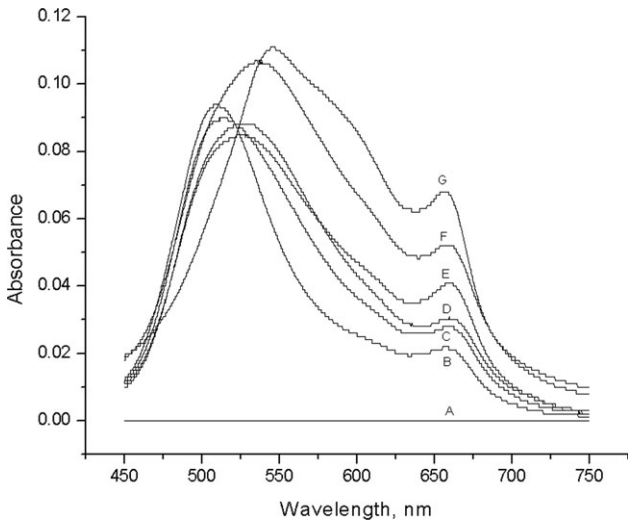

Figure 5. Absorbance spectra of MB in THF in the presence of different concentrations (mg mL^{-1}) of PS_{699}-*b*-$P(MMA_{232}/MAA_{58})$. A: 0.00; B: 0.04; C: 0.06; D: 0.14; E: 0.20; F: 0.24; G: 0.28; H: 0.32.

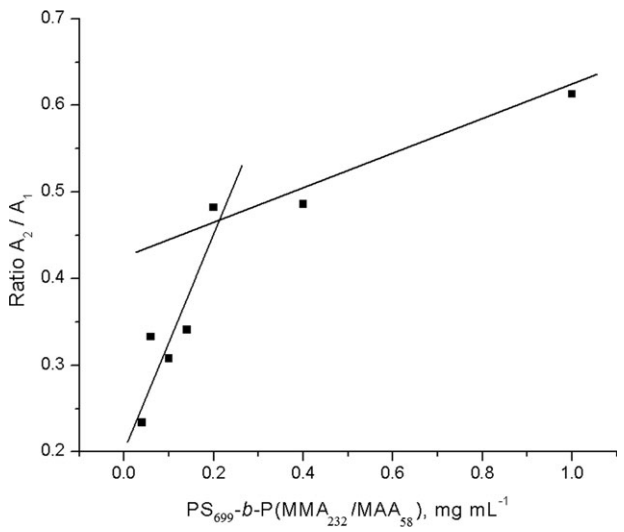

Figure 6. Plot of the ratio A_2/A_1 against the concentration of PS_{699}-*b*-$P(MMA_{232}/MAA_{58})$. The breaking point is attributed to the CMC.

Applied Polymer SCIENCE

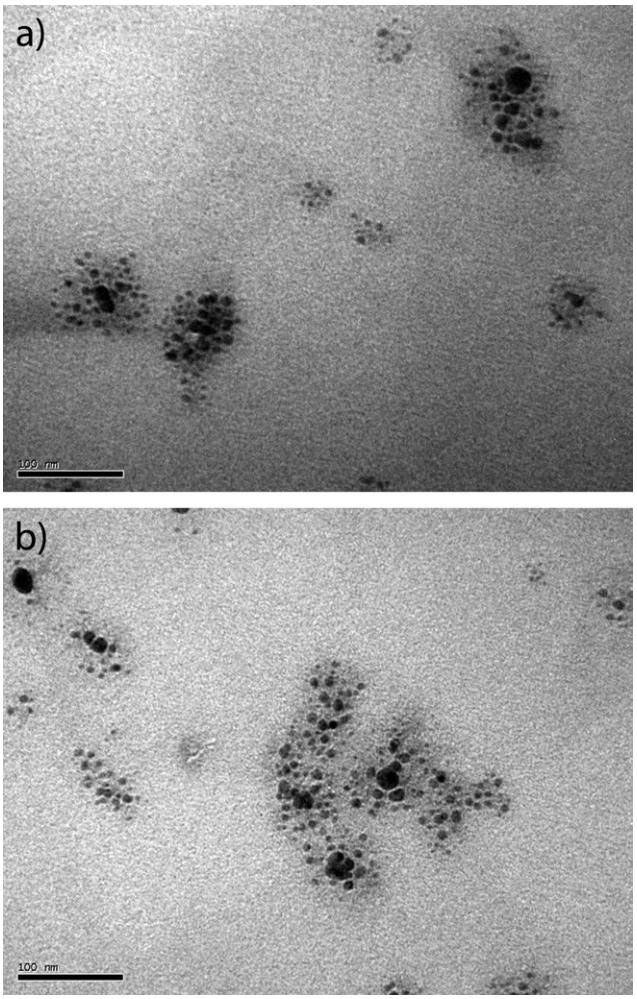

Figure 7. TEM micrographs PS_{699}-*b*-$P(MMA_{232}/MAA_{58})$ (a, b).

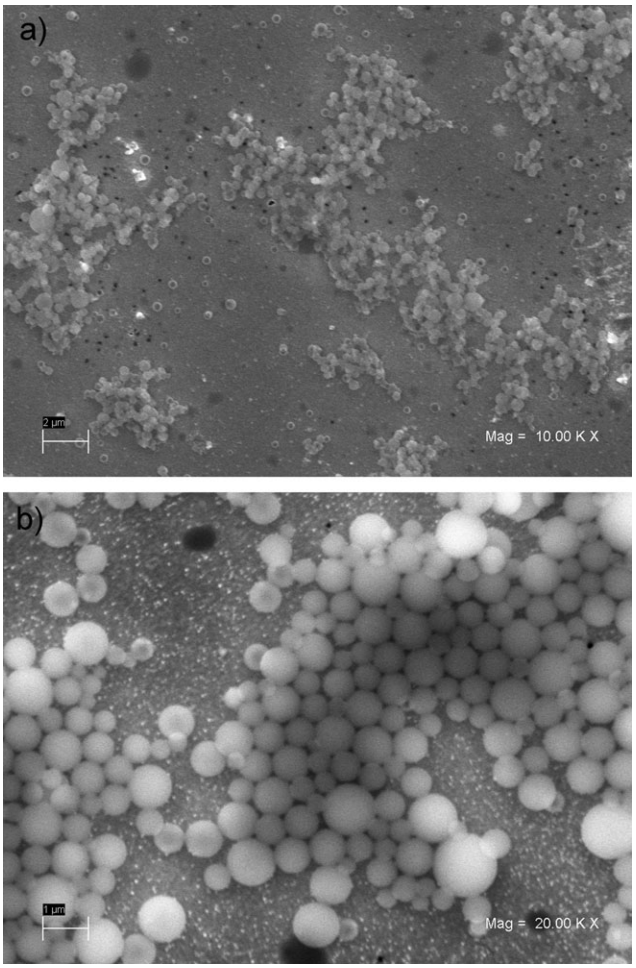

Figure 8. SEM micrographs of PS_{699}-*b*-$P(MMA_{232}/MAA_{58})$ (a, b).

attributed to the decomposition of the PMAA segment, was observed in the range of 100–150°C, whereas the second step was observed above 380°C.

The T_gs of PS–Br and both copolymers were examined by DSC under a nitrogen atmosphere. DSC curves obtained over the second heating cycles are shown in Figure 4. The curves reveal that all polymers presented a phase transition behavior corresponding to that of amorphous polymers. For PS–Br, a single T_g was observed at 85°C, whereas for PS_{699}-*b*-$PMMA_{290}$ at least two transitions are observed in the range of 105–115°C. The most important signal appearing at 106°C should correspond to the PS block and the small one to the PMMA block. These values are slightly shifted compared to the T_g values reported for PS (calculated, 99–102; experimental, 85–102) and PMMA (calculated, 85–105; experimental, 104–105).[22] This behavior could be attributed to the length of each block in the copolymer.

Interestingly, for PS_{699}-*b*-$P(MMA_{232}/MAA_{58})$, where 20% of MMA groups have been hydrolyzed to MAA, the value of T_g was shifted to a much lower value, that is 65°C. As a comparison, the T_g value of PMAA is 228°C. This huge difference, induced by a small structural change, can be explained in terms of bulk segregation of the modified block, $P(MMA_{232}/MAA_{58})$. The microstructure of the amphiphilic copolymers became affected by the presence of microdomains that were chemically distinct. The chemical link between different blocks prevented phase separation on the macroscopic scale, but allowed microphase separation of the two blocks, leading to self-assembled morphologies of the minority polymer block.

Self-aggregation and Morphological Behavior of PS_{699}-*b*-$P(MMA_{232}/MAA_{58})$

One of the most interesting properties of amphiphilic block copolymers is their ability to self-assemble into a large variety of micellar structures.[23] In this case, the formation of reverse micelles by PS_{699}-*b*-$P(MMA_{232}/MAA_{58})$ in organic solvents was driven by the repulsive interaction between the nonpolar solvent and the MAA groups in the hydrolyzed PMMA block. The size of the resultant micelles could be determined by structural parameters of the block copolymer.[23]

The self-aggregation of PS_{699}-*b*-$P(MMA_{232}/MAA_{58})$ in organic solvents has been monitored by UV spectroscopy using MB as the absorption probe. MB is a cationic dye whose absorption spectrum in polar solvents exhibits a maximum at 666 nm and a shoulder at 615 nm.[23,24] The latter absorption is attributed to

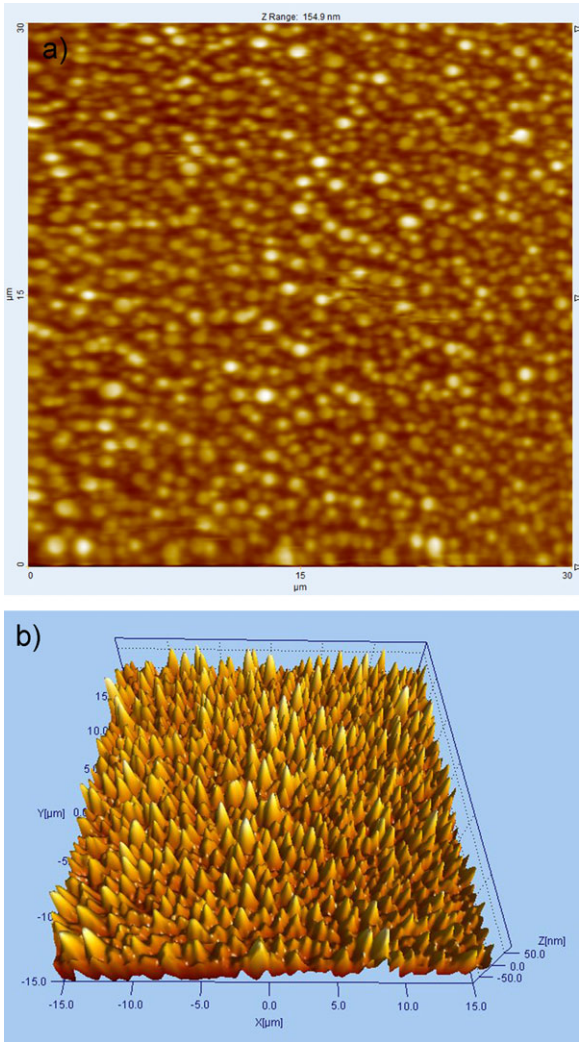

Figure 9. AFM images of PS_{699}-*b*-P(MMA_{232}/MAA_{58}). The scanning area was 30 μm × 30 μm, and the concentration was 0.1 mg mL^{-1} (a,b). [Color figure can be viewed in the online issue, which is available at wileyonlinelibrary.com.]

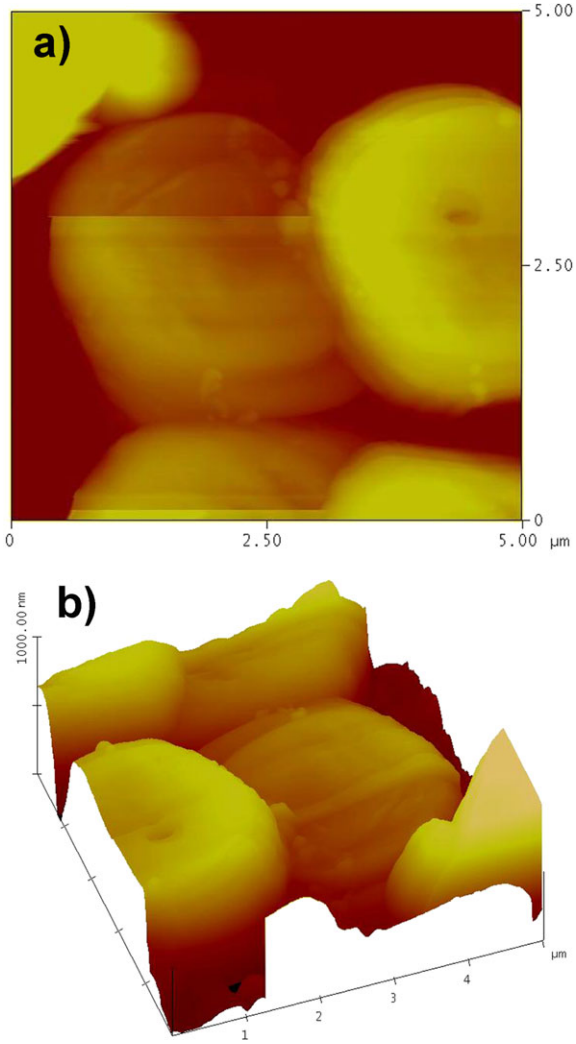

Figure 10. AFM images of the PS_{699}-*b*-P(MMA_{232}/MAA_{58}). The scanning area was 5 μm × 5 μm, and the concentration was 0.1 mg mL^{-1} (a,b). [Color figure can be viewed in the online issue, which is available at wileyonlinelibrary.com.]

a dimeric ion which is formed in solvents of high dielectric constant. In aqueous solution, it has been shown that the dimer formation is enhanced by cooperative binding of MB to negatively charged polyelectrolytes, and consequently the maximum of the dimer band shifts from 610 nm to lower wavelengths (up to 570 nm).[24]

In nonpolar solvents, the solubility of MB is quite low, but in the presence of nonionic surfactants, at concentrations above the critical micelle concentration (CMC), a new absorption band appears at 525 nm. This large blue shift has been attributed to the formation of a complex between the MB and the surfactant molecule.[25] Thus, MB has been used as an absorption probe in the study of nonionic reverse micelles,[24–26] and ionic liquid microemulsion.[26,27] As shown in Figure 5, the absorption spectrum of MB in THF, which appears only in the presence of PS_{699}-*b*-P(MMA_{232}/MAA_{58}), exhibits a maximum in the range of 510–547 nm (A_1) and a small absorption at 658 nm (A_2). These absorption bands can be attributed to a dimer formed by cooperative stacking of the dye onto the hydrophilic or polar segment of the copolymer (A_1)[28] and to monomer MB dissolved in the polar environment provided by the block copolymer (A_2). The ratio between monomer and dimer absorbances (A_2/A_1) is a measure of the relative concentration of these two MB forms. A plot of A_2/A_1 against concentration of PS_{699}-*b*-P(MMA_{232}/MAA_{58}) is shown in Figure 6. As both absorbances increase with polymer concentration, the increase of the ratio A_2/A_1 reflects the increases of the monomer form of MB. This behavior can be explained in terms of polymer aggregation, and therefore the plot in Figure 6 can be used to determine the CMC of the copolymer. The CMC obtained from the intersection of the linear parts of this plot is 0.20 mg mL^{-1}. The CMC determines the thermodynamic stability of the micelles.

The morphological properties of the micelles formed by this copolymer were investigated by DLS, TEM, SEM, and AFM. DLS

measurements of copolymer solutions in THF (1 mg mL^{-1}) showed that the size dispersion of the polymer micelles was relatively narrow ($Đ = 0.436$) with an effective particle diameter of 79.9 nm. This size range suggests that these micelles tended to aggregate, thereby forming larger structures. On the other hand, TEM images of PS_{699}-*b*-P(MMA_{232}/MAA_{58}) in THF (with drops of methanol) showed that large spherical aggregates with an average size of ~120 nm, probably consisting of a P(MMA_{232}/MAA_{58}) core surrounded by a PS corona were formed [Figure 7(a,b)]. Similar results were obtained by SEM of the polymer micelles formed by PS_{699}-*b*-P(MMA_{232}/MAA_{58}) in THF. In this case, large spherical aggregates were observed in the micrographs [Figure 8 (a,b)]. The driving force for aggregation was attributed to the amphiphilic nature of the block copolymer that raises repulsive interaction between the solvent and the more polar block.

The size dispersion of observed nanoparticles by DLS at a higher concentration was found to be relatively narrow ($Đ = 0.436$) with an effective particle diameter of 129.9 nm. These results suggest that the self-assemble copolymer form larger compound micelles, which finally predominated.[22]

The AFM micrographs of PS_{699}-*b*-P(MMA_{232}/MAA_{58}) showed that its surface morphology was a rough and ordered nanostructure in which nano-islands of various sizes (range, 96.8–159.2 nm) coexisted (Figure 9). This morphology suggests that phase segregation of amphiphilic copolymers induced the formation of large-scale phase nano-aggregates ($R_q = 124.3$ nm) (Figure 10).

CONCLUSIONS

An amphiphilic diblock copolymer, the PS_{699}-*b*-P(MMA_{232}/MAA_{58}), with a well-controlled structure has been synthesized through a two-stage ATRP method followed by partial hydrolysis of the MMA block. PS–Br, obtained in bulk by reverse ATRP, was used as a macroinitiator to polymerize MMA, and thus yielding PS_{699}-*b*-$PMMA_{290}$. Both the macroinitiator and the block copolymer were obtained with relatively low dispersity ($Đ$ =1.28 and 1.30, respectively). The thermal behavior showed that PS–Br decomposed in a single step, whereas the block copolymers exhibited a two-step degradation. In any case, the amphiphilic copolymer was less stable than its precursor. The first step observed in the range of 100–150°C was attributed to the P(MMA/MAA) segment.

Moreover, single T_gs were found for PS–Br (85°C) and for PS_{699}-*b*-P(MMA_{232}/MAA_{58}) (65°C), whereas for PS_{699}-*b*-$PMMA_{290}$ at least two transitions are observed in the range of 105–115°C. The decrease in T_g of the amphiphilic block copolymer was attributed to a change in its microstructure induced by segregation of the modified PMMA block.

The aggregation behavior of PS_{699}-*b*-P(MMA_{232}/MAA_{58}) in organic solvents has been monitored by UV absorption probing, and the CMC in THF was found to be 0.20 mg mL^{-1}. Both self-assembled and aggregated substances, in solution as well as in the form of films, were confirmed by TEM, SEM, and AFM. In solution, large spherical aggregates, consisting probably of a P(MMA/MA) core surrounded by a PS corona, were formed with an average size of ~120 nm. The increase in the surface roughness, observed by AFM, indicates a large-scale phase segregation under these conditions. The driving force for aggregation was attributed to the repulsive interaction between the nonpolar solvent and the methacrylic acid groups in the PMMA/MAA block.

ACKNOWLEDGMENTS

The authors gratefully acknowledge the support provided by the FONDECYT Grant 1110836, a UTEM Grant, Universidad Andrés Bello DI-44-10/R, and by the WCU Program funded by the Ministry of Education, Science, and Technology through the National Research Foundation of Korea (R31-10026).

REFERENCES

1. Matyjaszewski, K.; Gnanou, Y.; Leibler, L. Macromolecules Engineering: Precise Synthetic, Materials Properties, Applications; Wiley-VCH: Weinheim, Germany, **2007**.
2. Rzayev, J.; Hillmyer, M. A. *Macromolecules* **2005**, *38*, 3.
3. Zalusky, A. S.; Olayo-Valles, R.; Wolf, J. H.; Hillmyer, M. A. *J. Am. Chem. Soc.* **2002**, *124*, 12761.
4. Oh, K. T.; Bronich, T. K.; Bromberg, L.; Hatton, T. A.; Kabanov, A. V. *J. Control. Release* **2006**, *115*, 9.
5. Choucair, A.; Soo, P. L.; Eisenberg, A. *Langmuir* **2005**, *21*, 9308.
6. Lu, Z.; Liu, G.; Phillips, H.; Hill, J. M.; Chang, J.; Kydd, R. A. *Nano Lett.* **2001**, *1*, 683.
7. Boontongkong, Y.; Cohen, R. E. *Macromolecules* **2002**, *35*, 3647.
8. Matyjaszewski, K.; Patter, T. E.; Xia, J. *J. Am. Chem. Soc.* **1997**, *119*, 674.
9. Huang, J. Y.; Pintauer, T.; Matyjaszewski, K. *J. Polym. Sci. Part A: Polym. Chem.* **2004**, *42*, 3285.
10. Lutz, J. F.; Jahed, N.; Matyjaszewski, K. *J. Polym. Sci. Part A: Polym. Chem.* **2004**, *42*, 1939.
11. Sarbu, T.; Lin, K. Y.; Ell, J.; Siegwart, D. J.; Spanswick, J.; Matyjaszewski, K. *Macromolecules* **2004**, *37*, 3120.
12. Chang, Y.; Prange, R.; Allcock, H. R.; Lee, S. C.; Kim, C. *Macromolecules* **2002**, *35*, 8556.
13. Masci, G.; Bontempo, D.; Tiso, N.; Diociaiuti, M.; Mannina, L.; Capitani, D., Crescenzi, V. *Macromolecules* **2004**, *37*, 4446.
14. Bouilhac, C.; Cloutet, E.; Taton, D.; Deffieux, A.; Borsali, R.; Cramail, H. *J. Polym. Sci. Part A: Polym. Chem.* **2009**, *47*, 197.
15. Nakano, M.; Deguchi, M.; Matsumoto, K.; Matsuoka, H.; Yamaoka, H. *Macromolecules* **1999**, *32*, 7437.
16. Wang, J. S.; Matyjaszewski, K. *Macromolecules* **1995**, *28*, 7572.
17. Xia, J.; Matyjaszewski, K. *Macromolecules* **1997**, *30*, 7692.
18. Wang, W.; Dong, Z.; Xia, P.; Zhang, Q. *Macromol. Rapid Commun.* **1998**, *19*, 647.
19. Wang, W.; Yan, D. *ACS Symp. Ser.* **2000**, *768*, 263.

20. Xia, J.; Matyjaszewski, K. *Macromolecules* **1999**, *32*, 5199.
21. Davis, K. A.; Charleux, B.; Matyjaszewski, K. *J. Polym. Sci. Part A: Polym. Chem.* **2000**, *38*, 2274.
22. Wypych, G.; Handbook of Polymer, ChemTec Publishing: Toronto, Canada, **2012**; pp 451.
23. Saito, R.; Akiyama, Y.; Ishizu K. *Polymer* **1999**, *40*, 655.
24. Qi, L. M.; Ma, J. M.; *J. Colloid Interface Sci.* **1998**, *197*, 36.
25. Pramanick, D.; Mukherjee, D. *J. Colloid Interface Sci.* **1993**, *157*, 131.
26. Garate, J. A.; Valenzuela, M. A.; Garate, M. P.; Olea, A. F. *Colloid Surf. A: Physicochem. Eng. Aspects* **2007**, *307*, 28.
27. Li, N.; Gao, Y. A.; Zheng, L. Q.; Zhang, J.; Yu, L.; Li, X. W. *Langmuir* **2007**, *23*, 1091.
28. Moreno-Villoslada, I.; Torres-Gallego, C.; Araya-Hermosilla, R.; Nishide, H.; *J. Phys. Chem. B* **2010**, *114*, 4151.